A robust source-independent full-waveform inversion

Xin Fu*, Kris Innanen
xin.fu1@ucalgary.ca

Abstract

Full-waveform inversion (FWI) can reconstruct high-resolution underground velocity and lithology structures even under complex geological backgrounds, and has been widely developed. But a reliable real-data inversion generally needs accurate source wavelet information, which is still one of the major challenges in FWI. In this paper, a robust source-independent FWI method is developed, which is demonstrated via synthetic tests of different starting models, different true models, different levels of random noises, and different types of source wavelets. It does not require any prior source wavelet information. It does not require an accurate starting model, even a 1D starting model is feasible to output an accurate wavelet estimate. It is stable for random noises. A good estimate of the source wavelet can be obtained from a poorly converged model based on the new proposed wavelet estimation equation. All in all, the performance of the new source-independent FWI in the synthetic data tests is close to that of the known-source-wavelet FWI.

Introduction

In this paper, we will propose a new source-independent method, which is based on the frame of the iterative estimation of source signature (IES) method but employs a new source wavelet estimation formula. It reserves the merit of easy operation of the conventional IES method but overcomes its demerit of requiring an accurate initial starting model. And the new method is more stable on noise. In the synthetic data test using the modified acoustic Marmousi model, the performance of the new source-independent method is similar to that of the KSW method.

Method

- Iterative estimate of source signature method (our method):

$$E(\boldsymbol{m}) = \frac{1}{2}||\mathbf{d}_{\text{obs}} - \mathbf{S}_{\text{syn}}||^2 = \frac{1}{2}||\mathbf{d}_{\text{obs}} - \mathbf{W}\mathbf{G}_{\text{syn}}||^2 \quad \text{(Frequency domain)}$$

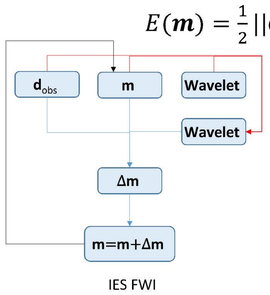

IES FWI

$$W = \frac{\mathbf{G}_{\text{syn}}{}^{\mathsf{T}}\mathbf{d}_{\text{obs}}{}^{*}}{\mathbf{G}_{\text{syn}}{}^{\mathsf{T}}\mathbf{G}_{\text{syn}}{}^{*}} = \frac{\sum_{i=1}^{n} \mathrm{G}_{\text{syn}}(\mathrm{i})\mathrm{d}_{\text{obs}}(\mathrm{i})^{*}}{\sum_{i=1}^{n} \mathrm{G}_{\text{syn}}(\mathrm{i})\mathrm{G}_{\text{syn}}(\mathrm{i})^{*}}$$ Old IES FWI

or

$$W = \frac{1}{n}\sum_{i=1}^{n} \frac{\mathrm{G}_{\text{syn}}(\mathrm{i})\mathrm{d}_{\text{obs}}(\mathrm{i})^{*}}{\mathrm{G}_{\text{syn}}(\mathrm{i})\mathrm{G}_{\text{syn}}(\mathrm{i})^{*}}$$ New IES FWI

i is trace number
Suppress noises from data noises, the inaccurate velocity model, and the imperfect forwarding modeling.

Numerical example

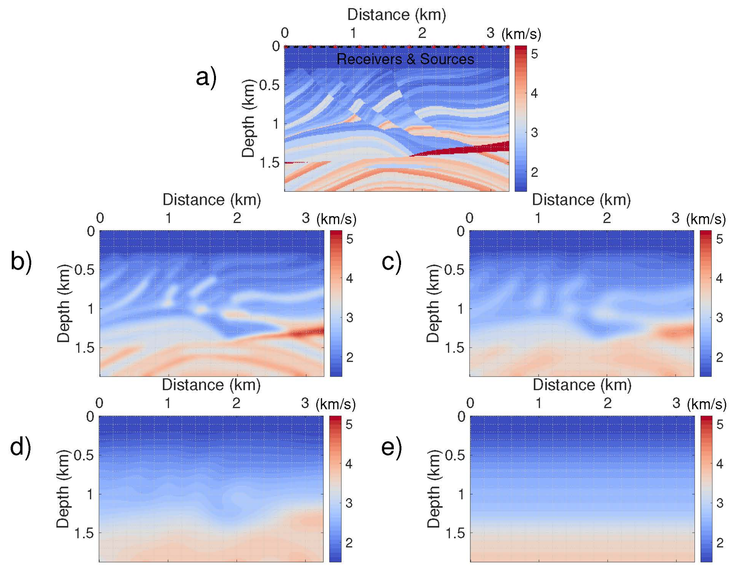

Figure: (a) True model (P-wave velocity) and acquisition geometries, (b) starting model 1, (c) starting model 2, (d) starting model 3, (e) starting model 4. Models 1 to 4 become smoother and smoother, and starting model 4 is 1D. The dash lines and asterisks in (a) are the locations of receivers and sources, respectively.

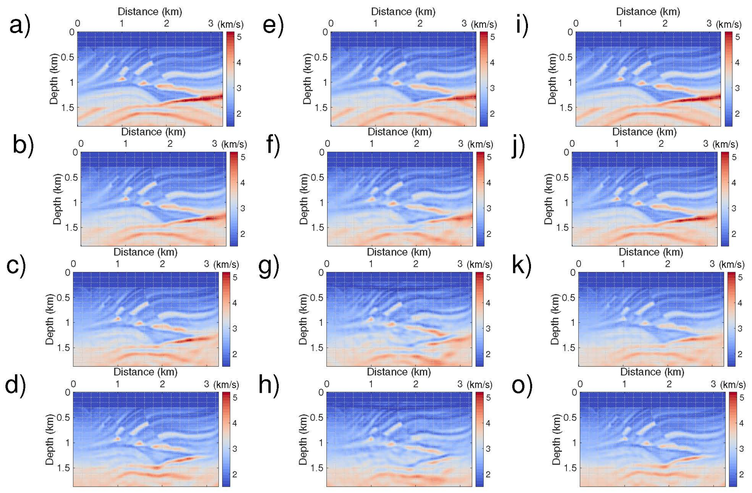

Figure: The first column is the final inverted results of the KSW method (using the true wavelet) using starting models 1 (a), 2 (b), 3 (c), and 4 (d), respectively. The second column is the final inverted results of the old method using starting models 1 (e), 2 (f), 3 (g), and 4 (h), respectively. The third column is the final inverted results of the new method using starting models 1 (i), 2 (j), 3 (k), and 4 (o), respectively.

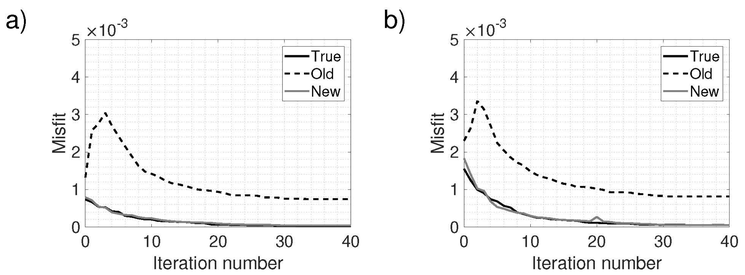

Figure: Curves of the data misfit versus the iteration number for different methods using starting models 1 (a) and 4 (d), respectively. In each panel, the black line is the data misfit curve for the KSW method, the dashed line is the data misfit curve of the old method, and the gray line is the data misfit curve of the new method.

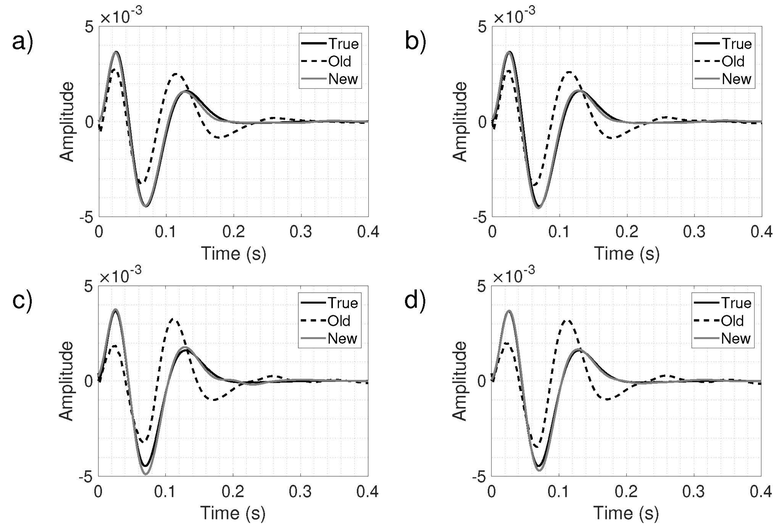

Figure: The final estimated source wavelets of the old method and the new method using starting models 1 (a), 2 (b), 3 (c), and 4 (d), respectively. In each panel, the black line is the true source wavelet, the dashed line is estimated from the old method, and the gray line is estimated from the new method.

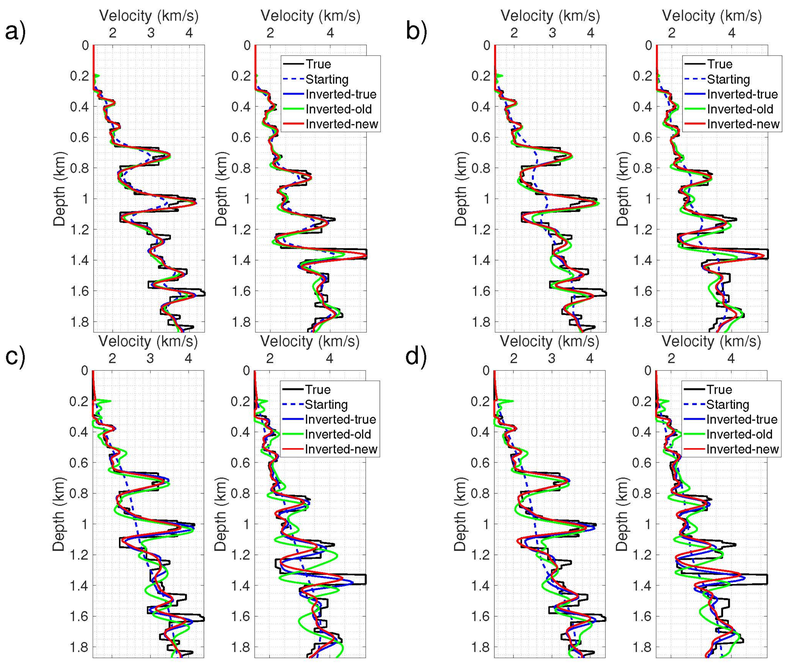

Figure: Traces extracted at distances 1.5km and 2.5km from the results shown in Figure 2. (a), (b), (c), and (d) are inverted traces of different methods using starting models 1, 2, 3, and 4, respectively. In each panel, the solid black line is the true model, the dashed blue line is the starting model, the solid blue line is the result of the KSW method, the solid green line is the result of the old method, and the solid red line is the result of the new method.

ACKNOWLEDGEMENTS

We thank the sponsors of CREWES for continued support. This work was funded by CREWES industrial sponsors, NSERC (Natural Science and Engineering Research Council of Canada) through the grants CRDPJ 543578-19.

NSERC CRSNG
UNIVERSITY OF CALGARY
FACULTY OF SCIENCE
Department of Geoscience